


## ORIGINAL ARTICLE

# Calcineurin B-like interacting protein kinase 31 confers resistance to sheath blight via modulation of ROS homeostasis in rice

Huan Chen<sup>1</sup> | QiuJun Lin<sup>1,2</sup> | Zhuo Li<sup>1</sup> | Jin Chu<sup>3</sup> | Hai Dong<sup>3</sup> | Qiong Mei<sup>1</sup> | Yuanhu Xuan<sup>1</sup> <sup>1</sup>College of Plant Protection, Shenyang Agricultural University, Shenyang, China<sup>2</sup>Institute of Agricultural Quality Standards and Testing Technology, Liaoning Academy of Agricultural Sciences, Shenyang, China<sup>3</sup>Institution of Plant Protection, Liaoning Academy of Agricultural Sciences, Shenyang, China**Correspondence**Qiong Mei and Yuanhu Xuan, College of Plant Protection, Shenyang Agricultural University, Shenyang 110866, China.  
Email: [meiqiong@syau.edu.cn](mailto:meiqiong@syau.edu.cn) and [xuanyuanhu115@syau.edu.cn](mailto:xuanyuanhu115@syau.edu.cn)**Abstract**

Sheath blight (ShB) severely threatens rice cultivation and production; however, the molecular mechanism of rice defence against ShB remains unclear. Screening of transposon *Ds* insertion mutants identified that *Calcineurin B-like protein-interacting protein kinase 31* (*CIPK31*) mutants were more susceptible to ShB, while *CIPK31* overexpressors (*OX*) were less susceptible. Sequence analysis indicated two haplotypes of *CIPK31*: Hap\_1, with significantly higher *CIPK31* expression, was less sensitive to ShB than the Hap\_2 lines. Further analyses showed that the NAF domain of *CIPK31* interacted with the EF-hand motif of respiratory burst oxidase homologue (*RBOHA*) to inhibit *RBOHA*-induced  $H_2O_2$  production, and *RBOHA RNAi* plants were more susceptible to ShB. These data suggested that the *CIPK31*-mediated increase in resistance is not associated with *RBOHA*. Interestingly, the study also found that *CIPK31* interacted with catalase C (*CatC*); *cipk31* mutants accumulated less  $H_2O_2$  while *CIPK31 OX* accumulated more  $H_2O_2$  compared to the wild-type control. Further analysis showed the interaction of the catalase domain of *CatC* with the NAF domain of *CIPK31* by which *CIPK31* inhibits *CatC* activity to accumulate more  $H_2O_2$ .

**KEYWORDS***CIPK31*, homeostasis, resistance, rice, ROS, sheath blight

## 1 | INTRODUCTION

*Rhizoctonia solani* causes sheath blight (ShB), a major threat to rice cultivation and production (Zheng et al., 2013). In recent years, the incidence area and yield loss due to ShB have been increasing in China (Qi et al., 2021); therefore, there is an urgent need to identify new genetic resources to support resistance breeding. Previous studies demonstrated that resistance against ShB is a trait controlled by multiple quantitative trait loci (QTLs). Researchers have

identified several QTLs and cloned a few (Eizenga et al., 2013; Pinson et al., 2005; Richa et al., 2016, 2017). In addition, studies have attempted to dissect the mechanisms of rice resistance against ShB (Molla et al., 2020). Our previous work showed that ethylene (ET) positively regulates rice resistance against ShB, while brassinosteroid (BR) signalling had a negative influence (Yuan et al., 2018). Several other studies have demonstrated the role of lignin in ShB resistance. Overexpression of pathogenesis-related protein 5 (PR5) family member *OsOSM1* improved ShB resistance (Xue et al., 2016).

Huan Chen, QiuJun Lin and Zhuo Li contributed equally to this work.

This is an open access article under the terms of the [Creative Commons Attribution-NonCommercial-NoDerivs](https://creativecommons.org/licenses/by-nc-nd/4.0/) License, which permits use and distribution in any medium, provided the original work is properly cited, the use is non-commercial and no modifications or adaptations are made.

© 2023 The Authors. *Molecular Plant Pathology* published by British Society for Plant Pathology and John Wiley & Sons Ltd.

Similarly, overexpression of the ET biosynthetic gene *OsACS2* enhanced ShB resistance (Helliwell et al., 2013). A rice and maize gene, *cinnamyl alcohol dehydrogenase* (*CAD*), responsible for lignin biosynthesis, also positively regulates rice resistance against ShB (Li et al., 2019). In addition, we found that INDETERMINATE DOMAIN (IDD) IDD14 and IDD13 activate *PIN1a* to promote ShB resistance (Sun et al., 2019a, 2020), and Dense and Erect Panicle 1 (*DEP1*) interacts with IDD14 to negatively regulate ShB defence (Liu et al., 2021). A recent study identified that RESISTANCE OF RICE TO DISEASES1 (*ROD1*) interacts with catalase B (*CatB*), modulates cellular  $H_2O_2$  levels, and controls ShB defence (Gao et al., 2021). However, the function of other catalases in rice resistance against ShB remains unknown.

Calcineurin B-like protein (CBL)-interacting protein kinases (CIPKs) play key roles in plant defence. In *Arabidopsis thaliana*, AtCIPK6 negatively regulates plant resistance to *Pseudomonas syringae* by modulating reactive oxygen species (ROS) production (Sardar et al., 2017). AtCIPK26 interacts with AtCBL1, and AtCBL9 phosphorylates the NADPH oxidase AtRBOHF and promotes ROS generation (Han et al., 2019). In wheat, TaCBL4-TaCIPK5 regulates ROS signalling and controls defence against stripe rust fungus (Liu et al., 2018). TaCIPK10 improves tolerance to stripe rust fungus by controlling ROS accumulation (Liu et al., 2019). In rice, OsCIPK14 and OsCIPK15 interact with OsCBL4 to regulate microbe-associated molecular pattern (MAMP)-mediated defence signalling (Kurusu et al., 2010). OsCIPK23 positively regulates rice blast resistance by controlling the cellular potassium levels (Shi et al., 2018). Our recent finding showed that CIPK31 promotes potassium uptake to increase rice resistance to blast disease (Lin et al., 2021). However, CIPK's role in rice defence against ShB has not been investigated.

We therefore isolated ShB-susceptible mutant *cipk31* from *Ds*-insertion mutant pools. We then examined the role of CIPK31 in generating ROS by analysing the six respiratory burst oxidase homologues, RBOHA, B, C, D, E, and H, and three catalases, CatA, CatB, and CatC. The results showed that CIPK31 inhibits both RBOHA and CatC to modulate ROS homeostasis, promoting rice resistance against ShB. In addition, CIPK31 promotes ROS levels, which confers a broad-spectrum resistance in rice. Thus, the paper shows that CIPK31 promotes rice resistance against ShB, exhibiting a great advantage in breeding for improved resistance.

## 2 | RESULTS

### 2.1 | CIPK31 positively regulates rice resistance against ShB

Previously, we screened ShB resistance/susceptibility genes using a transposable element *Ds* insertion mutant pool (Sun et al., 2019b) (Figure 1a). We identified two *cipk31* mutants with an insertion in the fourth (*cipk31-1*) and 11th (*cipk31-2*) exons, respectively; these *cipk31* mutants showed no *CIPK31* expression (Figure 1b). Inoculation with *Rhizoctonia solani* AG1-IA showed that *cipk31* mutants were more

susceptible to ShB than the wild-type Dongjin (DJ) (Figure 1c-f). To further investigate the *CIPK31* function, *CIPK31* overexpression (OX) plants were generated in the Zhonghua 11 (ZH11) background. The *CIPK31* expression level was significantly higher in these *CIPK31* OXs (#1-#5) than in ZH11 (Figure 2a). Moreover, these *CIPK31* OX lines (#1, #4) were less susceptible to ShB as evaluated by inoculation with *R. solani* AG1-IA to leaves (Figure 2b,c) and sheaths (Figure 2c,d).

Analysis of the natural variation in *CIPK31* revealed that the genomic sequences were divided into two haplotypes (Haps). Except for a few single-nucleotide polymorphisms (SNPs) in the promoter and exons, Hap\_2 had deletions in the promoter region. At location 11,527,010 on rice genome, base C in Hap\_1 and T in Hap\_2, the SNP difference does not cause amino acid change. Similarly, at location 11,527,188, base G in Hap\_1 and A in Hap\_2, which does not cause amino acid change either (Figure 3a). Reverse transcription-quantitative PCR (RT-qPCR) showed that the *CIPK31* level was significantly higher in the five cultivars belong to Hap\_1 (JRC003, Beigeng2, Longdao18, B001, and B003) than in the five cultivars belong to Hap\_2 (Amane, ARC10633, Djimoron, Qishanzhan, Bakiella1) (Figure 3b). Inoculation of *R. solani* AG1-IA revealed that Hap\_1 cultivars were less susceptible to ShB than Hap\_2 varieties (Figure 3c,d).

### 2.2 | CIPK31 interacts with RBOHA and inhibits its function

To investigate the molecular mechanism of underlying CIPK31-mediated regulation of rice resistance, CIPK31 interaction proteins were screened by yeast two-hybrid assay. Among the interactors, the N-terminal region of RBOHA showed interaction with CIPK31 but not the other RBOHs (RBOH B-F; Figure S1a). The open-source AF2 complex (<https://github.com/FreshAirTonight/af2complex>) predictive analysis system was used to predict the CIPK31-RBOHA interaction model (Gao et al., 2022). The result showed that the NAF domain of CIPK31 interacts with the EF-hand motif of RBOHA (Figure S1b,c). The expression of RBOHA significantly increased  $H_2O_2$  levels; however, the coexpression of CIPK31 and RBOHA inhibited RBOHA-induced  $H_2O_2$  accumulation (Figure S1d). Therefore, to test RBOHA function in rice resistance against ShB, RBOHA RNA interference (RNAi) lines were generated in the ZH11 background. RT-qPCR showed significant suppression in RBOHA levels in the RBOHA RNAi plants (#1, #2) (Figure S1e). Inoculation of *R. solani* AG1-IA revealed that RBOHA RNAi plants (#1, #2) were more susceptible to ShB than ZH11 (Figure S1f,g).

### 2.3 | CIPK31 interacts with CatC to increase cellular $H_2O_2$ levels

Further analysis showed that *CIPK31* OXs accumulated more  $H_2O_2$  while *cipk31* mutants accumulated less than their corresponding wild-type plants (Figure 4a,b). The results suggested that CIPK31 interacts with RBOHA and inhibits RBOHA-mediated induction of

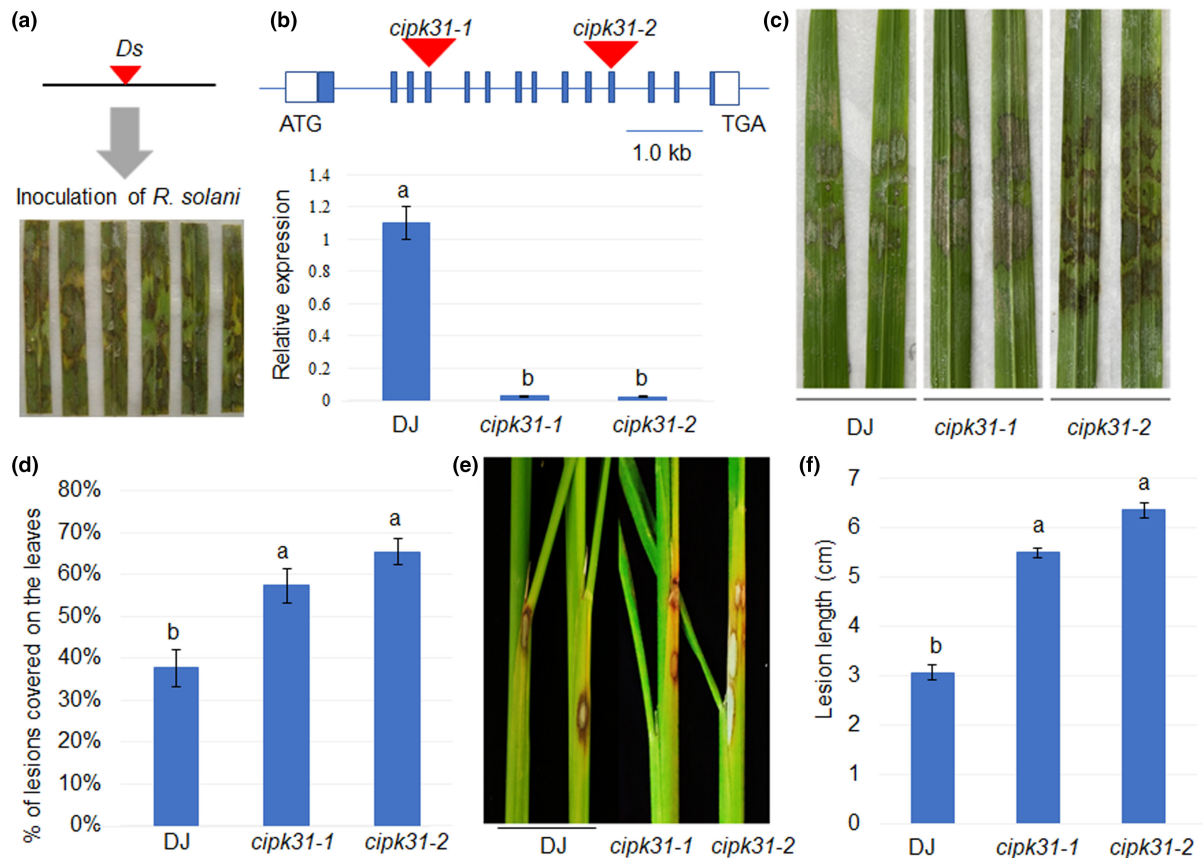


**FIGURE 1** *cipk31* mutants are more susceptible to sheath blight. (a) *Ds* insertion mutants inoculated with *Rhizoctonia solani* AG1-IA. (b) *Ds* insertions in *cipk31-1* and *cipk31-2* mutants. Blue and white boxes indicate exons and untranslated regions, respectively; the red triangles indicate *Ds*. *CIPK31* expression levels in Dongjin (DJ), *cipk31-1*, and *cipk31-2* plants. (c) DJ, *cipk31-1*, and *cipk31-2* leaves inoculated with *R. solani* AG1-IA. (d) The percentage of lesions on leaves shown in (c). (e) DJ, *cipk31-1*, and *cipk31-2* sheaths inoculated with *R. solani* AG1-IA. (f) The length of lesions on the sheaths shown in (e). Different lowercase letters indicate significant differences at  $p < 0.05$

ROS production, and RBOHA positively regulates rice resistance against ShB (Figure S1). We tested other interactors and found that CatC but not CatA and CatB interacted with CIPK31 (Figure 4c). CatB and CatC are localized in the peroxisome, with punctuated localization in the cells (Gao et al., 2021; You et al., 2022). The present study localized GFP-CatC in the punctuated cellular compartment and CIPK31-RFP mainly in the cytosol, while they localized together in the punctuated cellular compartment (Figure 4d). A bimolecular fluorescence complementation (BiFC) assay showed that CatC interacted with CIPK31 in the punctuated cellular compartment (Figure 4e), and a yeast two-hybrid assay showed that the CIPK31 C-terminal interacted with CatC (Figure 5a). The interaction between CIPK31 and CatC was predicted by the open-source AF2 complex (<https://github.com/FreshAirTonight/af2complex>) predictive analysis system (Gao et al., 2022). Structure simulation revealed that the NAF domain of CIPK31 interacts with the catalytic domain of CatC (Figure 5b). Functional analysis showed that *CIPK31* OXs had lower catalase activity while *cipk31* mutants exhibited higher activity than their corresponding wild-type plants (Figure 5c,d). To clarify whether NAF interacts with CatC to inhibit catalase activity, glutathione S-transferase (GST) or recombinant NAF-GST proteins were expressed in *Escherichia coli*. First, 100, 200, and 500 ng of GST

or NAF-GST proteins (Figure 5e) were added into the *CatC*-Myc OX plant total protein extracts. Western blot analysis results detected increasing levels of GST or NAF-GST in *CatC*-Myc OX plant total protein extracts with the addition of the recombinant proteins, while similar levels of *CatC*-Myc were detected in each treatment group (Figure 5f). Catalase activity measurement showed that addition of GST protein did not affect catalase activity, but the degree of the activity inhibition increased as the concentration of NAF-GST increased (Figure 5g).

We further generated *CatC* RNAi and OX plants to evaluate *CatC* function. *CatC* expression levels were significantly higher in *CatC* OX plants than in the wild-type ZH11 (Figure 6a). Inoculation of *R. solani* AG1-IA revealed that *CatC* OXs were more susceptible to ShB than the wild-type plants (Figure 6b,c); the catalase activity was much higher in *CatC* OXs than in wild-type ZH11 (Figure 6d). *CatC* expression levels were significantly lower in *CatC* RNAi plants than in the wild-type ZH11 (Figure 6e). Inoculation of *R. solani* AG1-IA revealed that *CatC* RNAi lines were less susceptible to ShB (Figure 6f,g); the catalase activity was much lower in *CatC* RNAi lines than in the wild-type ZH11 (Figure 6h).

Because cellular ROS levels are associated with broad-spectrum resistance in rice, the resistance of *cipk31* and *CIPK31* OX plant to

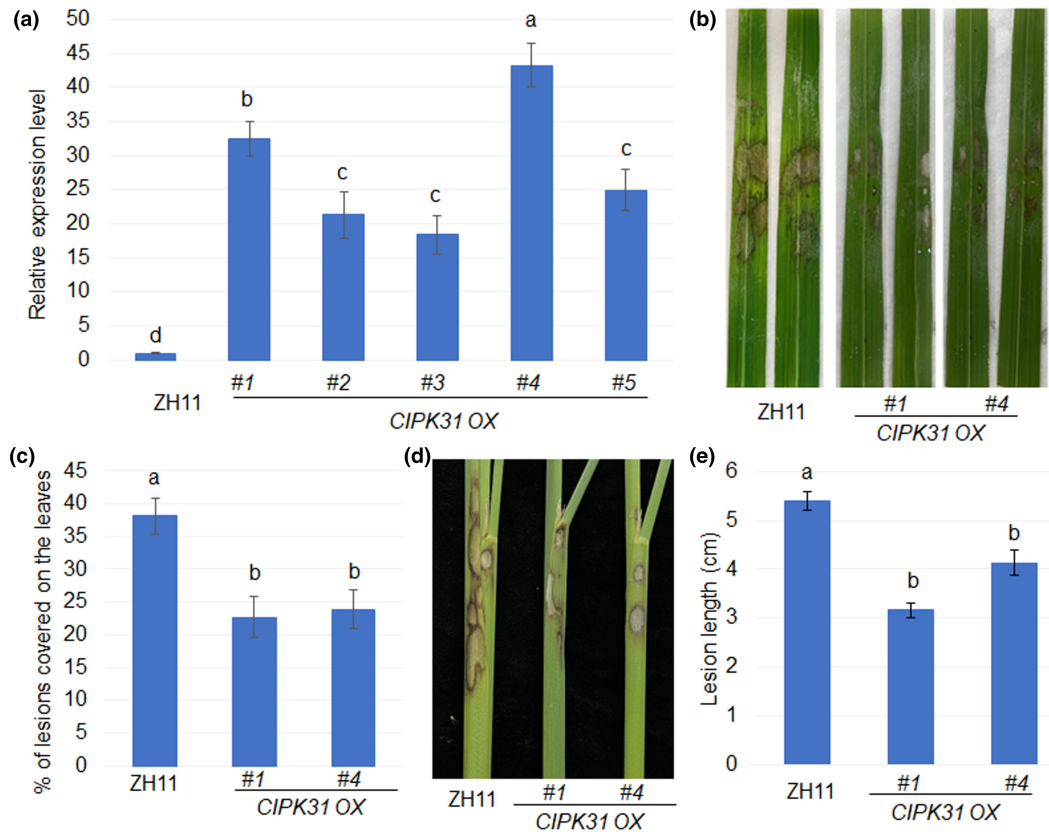


**FIGURE 2** *CIPK31* overexpressing (OX) plants are less susceptible to sheath blight. (a) *CIPK31* expression levels in Zhonghua 11 (ZH11) and *CIPK31* overexpressing plants (*CIPK31* OX#1 to #5). (b) ZH11 and *CIPK31* OXs (#1, #4) leaves inoculated with *Rhizoctonia solani* AG1-IA. (c) The percentage of lesions on leaves shown in (b). (d) The sheaths of ZH11 and *CIPK31* OXs (#1, #4) inoculated with *R. solani* AG1-IA. (e) The length of lesions on the sheaths shown in (d). Different lowercase letters indicate significant differences at  $p < 0.05$

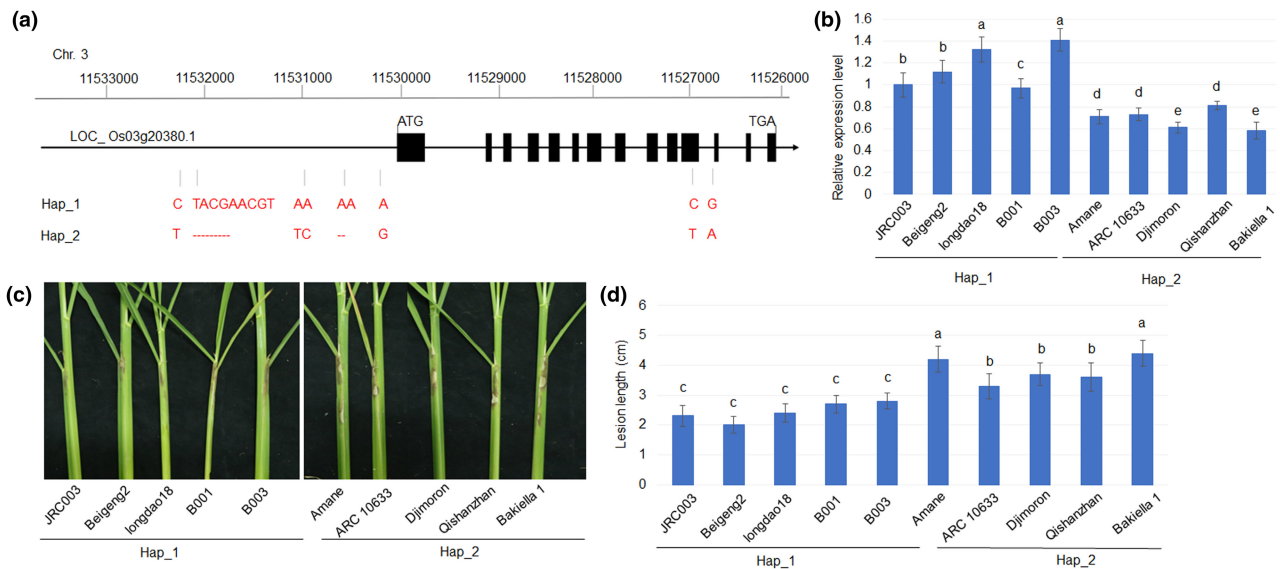


**FIGURE 3** Gene expression and sheath blight defence in *CIPK31* haplotypes. (a) The physical map of the *CIPK31* genomic region. The number on the top of the map indicates the physical location, and the sequence differences of Hap\_1 and Hap\_2 are shown below the map. Red dotted lines indicate nucleotide deletions. (b) *CIPK31* expression levels in the Hap\_1 and the Hap\_2 cultivars. (c) Sheaths of Hap\_1 and the Hap\_2 cultivars inoculated with *Rhizoctonia solani* AG1-IA. (d) The length of lesions on the sheaths shown in (c). Different letters indicate significant differences between the cultivars at  $p < 0.05$



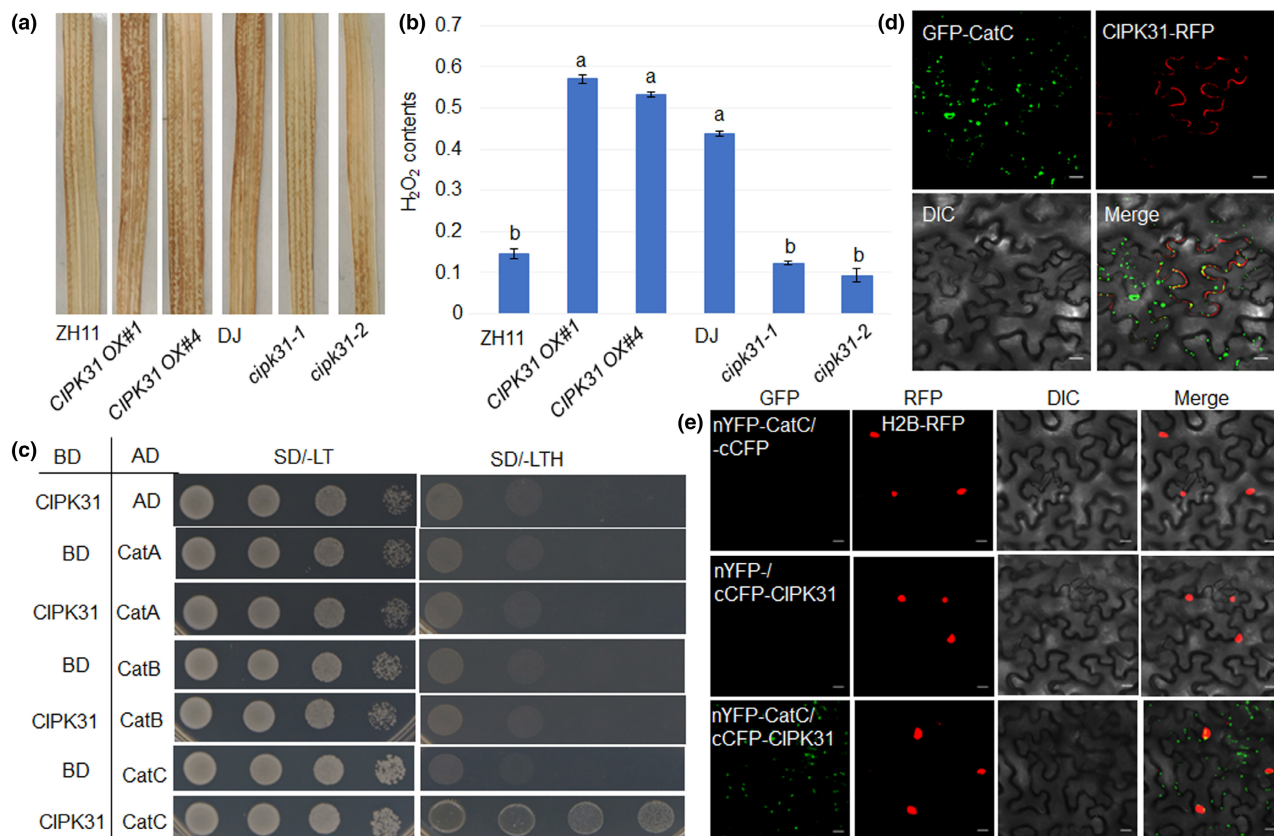


**FIGURE 4** CIPK31 interacts with CatC to accumulate cellular H<sub>2</sub>O<sub>2</sub>. (a) 3,3'-diaminobenzidine staining of Zhonghua 11 (ZH11), CIPK31 overexpression lines (OXs) (#1, #4), wild-type Dongjin (DJ), *cipk31-1*, and *cipk31-2* leaves. (b) H<sub>2</sub>O<sub>2</sub> content in ZH11, CIPK31 OXs (#1, #4), DJ, *cipk31-1*, and *cipk31-2* leaves. (c) Yeast two-hybrid assay for CIPK31 interactions with CatA, CatB, and CatC. (d) Colocalization of GFP-CatC and CIPK31-RFP in *Nicotiana* leaves. The figure shows the GFP, RFP, differential interference contrast (DIC), and merged images. (e) Bimolecular fluorescence complementation assay for CIPK31 and CatC interaction. nYFP-CatC+cCFP, nYFP+cCFP-CIPK31, or nYFP-CatC+cCFP-CIPK31 were coexpressed in *Nicotiana* leaves, and YFP reconstruction was examined. Bar = 20 μm

rice blast and bacterial blight were examined. Inoculation with *Magnaporthe grisea* strain Guy11 showed that *cipk31* was more susceptible while CIPK31 OX was less susceptible to rice blast than their wild-type plant (Figure S2a–d). The *cipk31* mutants were more sensitive, while CIPK31 OXs were less susceptible to *Xanthomonas oryzae* pv. *oryzae* PXO<sup>86</sup>, causing bacterial blight, than the wild-type plant (Figure S2e–h).

### 3 | DISCUSSION

ShB severely affects rice production, but the defence mechanism against ShB still remains largely unknown. We previously used 300 rice *Ds*-insertion mutants to isolate ShB resistance/susceptibility genes (Sun et al., 2019b), which are useful genetic resources for ShB resistance breeding in rice. Among the *Ds*-insertion lines, *cipk31* mutants were more susceptible to ShB (Figure 1), while CIPK31 OX showed an opposite phenotype (Figure 2), indicating that CIPK31 positively regulates rice resistance against ShB. Natural variations in CIPK31 sequences revealed the presence of two haplotypes of CIPK31 among the rice resources (Wang et al., 2018). Hap<sub>1</sub> and

Hap<sub>2</sub> showed differences in the sequences of the promoter and exon regions, including SNPs and indel. The two SNPs in the exon did not change the encoded amino acid (Figure 3a). Dongjin (DJ) and Zhonghua 11 (ZH11) belong to Hap<sub>1</sub> type. The CIPK31 expression level was significantly lower in the Hap<sub>2</sub> cultivars than in the Hap<sub>1</sub> cultivars (Figure 3b), which might be caused by deletions in the promoter region of the Hap<sub>2</sub> type cultivars. The Hap<sub>2</sub> cultivars were less susceptible to ShB than the Hap<sub>1</sub> cultivars (Figure 3c,d), suggesting a positive association between CIPK31 expression and rice resistance against ShB.

3,3'-diaminobenzidine (DAB) staining and H<sub>2</sub>O<sub>2</sub> measurement indicated that cellular H<sub>2</sub>O<sub>2</sub> levels were positively associated with the CIPK31 expression level. RBOHA, an NADPH oxidase that synthesizes extracellular superoxide (Groom et al., 1996), was identified as an interactor of CIPK31 in the study. Further examination revealed that the C-terminal of CIPK31 interacts with the second EF-hand motif (a Ca<sup>2+</sup>-binding motif) (Hao & Rasmusson, 2016) of RBOHA. Structure simulation implied interaction between the NAF domain of CIPK31 and the EF-hand motif of RBOHA. In tobacco leaves, the co-expression of CIPK31 and RBOHA inhibited RBOHA-induced H<sub>2</sub>O<sub>2</sub> levels, suggesting that CIPK31 interacts with and inhibits RBOHA

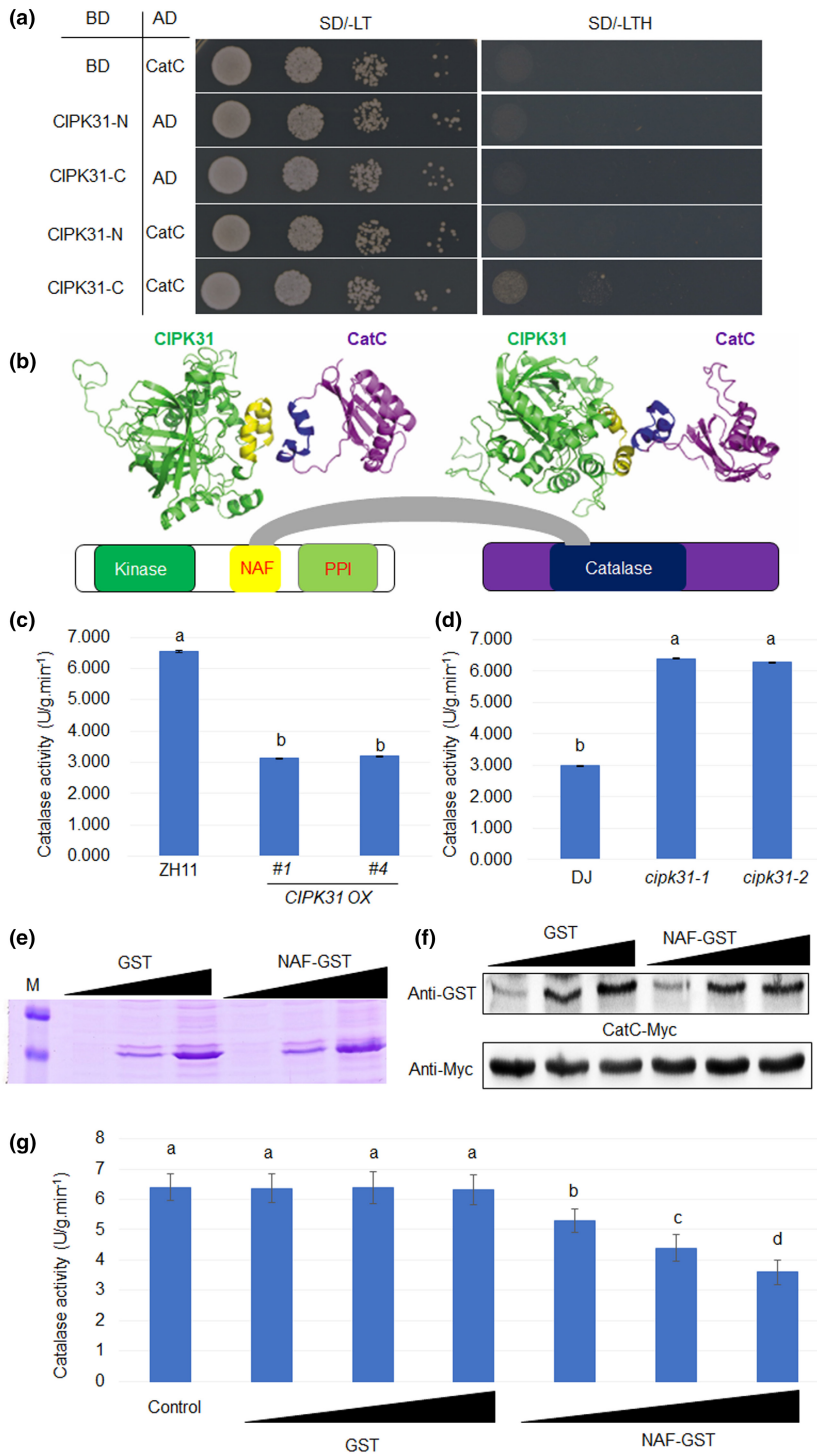


**FIGURE 5** CIPK31 C-terminal interacts with CatC to inhibit its function. (a) Yeast two-hybrid assays for interactions between CatC and N- or C-terminal of CIPK31. (b) Structure simulation of CIPK31 and CatC interaction. CIPK31 NAF domain interacts with catalase domain. Catalase activity in Zhonghua 11 (ZH11) and *CIPK31* overexpression lines (OXs) (#1, #4) (c) or wild-type Dongjin (DJ), *cipk31-1*, and *cipk31-2* plants (d). (e) SDS PAGE loading of glutathione S-transferase (GST) or NAF-GST recombinant proteins. Black triangle indicates the protein concentration gradient. M, marker. (f) Western blot analysis for GST or NAF-GST or CatC-Myc levels in CatC-Myc expression plant extract with addition of increasing amounts of GST or NAF-GST recombinant proteins. (g) Catalase activity in CatC-Myc expression plant extract (control) or in the samples with addition of GST or NAF-GST recombinant proteins. Different lowercase letters indicate significant differences at  $p < 0.05$

function. A previous study also reported that  $\text{Ca}^{2+}$  addition to the membrane protein fraction activated ROS generation, implying that the RBOH EF-hand motif might bind with  $\text{Ca}^{2+}$  to activate its enzyme activity (Nagano et al., 2016) and induce an ROS burst, maintaining immune homeostasis during plant-microbe interaction (Yuan et al., 2017). These findings implied that the CIPK31 NAF domain might interact with the EF-hand motif to inhibit  $\text{Ca}^{2+}$  binding, hindering RBOHA activity. In addition, the study found that *ROBHA* mutants were more susceptible to ShB, while *CIPK31* OX plants were

resistant to ShB, suggesting that CIPK31 might activate defence via other mechanisms.

Interestingly, CatC, not CatA and CatB, interacted with CIPK31, indicating that CIPK31 specifically regulates CatC. Generally, catalases, localized in the peroxisome, catabolize  $\text{H}_2\text{O}_2$  to  $\text{H}_2\text{O}$  and oxygen (Tung et al., 2015). *CatB* mutants showed a broad-spectrum resistance in rice (Gao et al., 2021). The CIPK31 NAF domain interacts with the catalase domain of CatC, by which CIPK31 inhibits catalase activity and the CatC-mediated

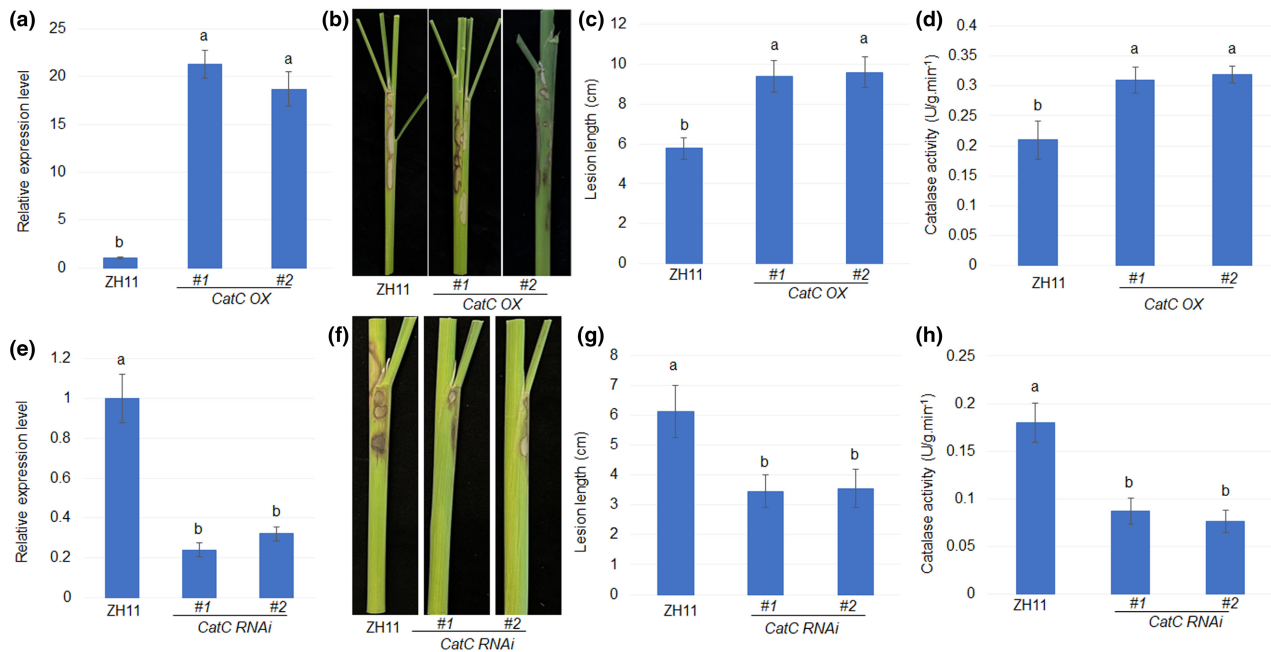


**FIGURE 6** CatC negatively regulates rice resistance against sheath blight. (a) CatC expression levels in Zhonghua 11 (ZH11) and CatC overexpression lines (OXs) (#1, #2). (b) Sheaths of ZH11 and CatC OXs (#1, #2) inoculated with *Rhizoctonia solani* AG1-IA. (c) The length of lesions on the sheaths shown in (b). (d) Catalase activity in ZH11 and CatC OXs (#1, #2). (e) CatC expression levels in ZH11 and CatC RNA interference (RNAi) plants (#1, #2). (f) Sheaths of ZH11 and CatC RNAi plants (#1, #2) inoculated with *R. solani* AG1-IA. (g) The length of lesions on the sheaths shown in (b). (h) Catalase activity in ZH11 and CatC RNAi plants (#1, #2). Different lowercase letters indicate significant differences at  $p < 0.05$

accumulation of cellular  $\text{H}_2\text{O}_2$ . A genetic study using CatC RNAi and CatC OX plants indicated that CatC negatively regulates rice resistance against ShB, but *R. solani* AG1-IA inoculation did not alter CIPK31 and RBOHA expression levels (Figure S3). Meanwhile, blast fungal inoculation highly induced RBOHA and RBOHB (Yang et al., 2017), suggesting that RBOHA might not be the primary NADPH oxidase acting in response to ShB. In addition, these data implicated CatC action over RBOHA in the production of ROS during *R. solani* infection.

Further analysis of the catalase activity and  $\text{H}_2\text{O}_2$  levels showed that CIPK31 inhibited CatC's ability to accumulate  $\text{H}_2\text{O}_2$  (Figures 4a–e and 5a–g), which might be the main regulatory mechanism by which CIPK31 controls rice resistance against ShB. CIPK23 and CIPK31 promote rice resistance to blast disease by activation of potassium uptake (Lin et al., 2021; Shi et al., 2018), but the potassium transporter mutant *akt1* contains less potassium in rice and is less susceptible to ShB (Yuan et al., 2020), implying a differential and complex regulatory mechanism of rice resistance to blast and ShB. Previously, a study found that the mutants of NOE1, which encodes CatC, accumulate and exhibit a programmed cell death phenotype (Lin et al., 2012). Meanwhile, RESISTANCE OF RICE TO DISEASES1 (ROD1) is known to interact with CatB to control cellular ROS levels and suppress the broad-spectrum resistance of rice; ROD1 interacts with CatA also (Gao et al., 2021). CatC was recently identified

as a target of E3 ligase APIP6, which regulates plant immunity (You et al., 2022). However, CIPK31 specifically interacts with CatC to provide resistance against rice blast (Lin et al., 2021), ShB (Figures 1a–f and 2a–e), and bacterial blight (Figure S2e–h), suggesting that CIPK31 promotes cellular ROS levels and provides broad-spectrum resistance.

In *Arabidopsis*, AtCIPK26 interacts with AtCBL1 and AtCBL9 at the plasma membrane, phosphorylates the NADPH oxidase AtRBOHF, and promotes ROS generation via a phosphorylation mechanism (Han et al., 2019). However, in this study, we identified that CIPK31 interacted with RBOHA or CatC via the NAF domain rather than a kinase domain (Figures 4, 5, and S1), suggesting a diverse regulatory mechanism of CIPKs in signal transduction. Further investigation is necessary to elucidate the significance of the interaction between the NAF domain of CIPK31 and the interactors. Because CIPK31 inhibits both RBOHA and CatC and promotes ROS levels, further genetic study with a combination of *rboha* × *catc* will be interesting to dissect the mechanism of CIPK31-mediated ROS homeostasis. Taken together, CIPK31 confers resistance to ShB (Figures 1a–f and 2a–e), rice blast (Lin et al., 2021), and bacterial blight (Figure S2e–h), and plays roles in growth and development in plants (Cho et al., 2019; Nagarjuna et al., 2016; Peng et al., 2018; Piao et al., 2010). However, clearly, CIPK31 interacts with CatC to modulate ROS homeostasis to promote rice resistance.

## 4 | EXPERIMENTAL PROCEDURES

### 4.1 | Plant growth and pathogen inoculation

The rice plants were grown in the glass cultivation room of Shenyang Agricultural University under controlled conditions at 24–30°C, 70% relative humidity, and 12 h light. Two-month-old *cipk31*, *CIPK31 OX*, *RBOHA RNAi*, *CatC RNAi*, *CatC OX*, and their corresponding wild-type plants were used for *R. solani* inoculation. The *R. solani* isolate AG1-1A was incubated on potato dextrose agar (PDA) at 26°C for 2–4 days before inoculation (Cao et al., 2021). A mycelium disk was put on the centre of the PDA covered with wood veneers for about 7 days. Wood veneers from outermost ring of of the culture medium plate covered with mycelium were placed onto rice sheaths. The incidence was investigated after 7 days. Mycelium disks were used for the leaf inoculation method. The severity of sheath blight was indicated by the area (inoculation on leaf) and the length (inoculation on sheath) of the lesion.

### 4.2 | RNA extraction and RT-qPCR

Total RNA was isolated from 1-month-old rice leaves using TRIzol reagent (Takara), and the genomic DNA contamination was removed using the RQ-RNase-free DNase (Promega). Complementary DNA was synthesized from the extracted RNA using a GoScript Reverse Transcription Kit (Promega) according to the manufacturer's instructions. The gene expression levels were determined using RT-qPCR performed with SYBR Green (Takara) on a CFX96 real-time PCR system (Bio-Rad), normalizing to *Ubiquitin* levels. A minimum of three biological replicates and three technical replicates were used for each analysis. The primers used for RT-qPCR are listed in Table S1.

### 4.3 | Protein extraction and western blot analysis

Leaf tissues collected from 1-month-old rice wild-type and *CIPK31 OX* plants were thoroughly ground in liquid nitrogen, and 4-week-old *Nicotiana benthamiana* leaves were used for transient expression. One gram of each sample was lysed with 200 µl of 2× SDS sample buffer to extract the proteins. Samples were then centrifuged at 13,000×g and 4°C for 20 min, and the supernatant was removed to a fresh tube. The protein content of the supernatant was quantified using modified Bradford protein assay kit (Sangon Biotech). The protein (20 µg) was separated on a 10% SDS-PAGE gel and electrotransferred onto Immobilon-P membrane (Millipore) for subsequent western blot analysis using the following primary antibodies: anti-GFP antibody (1:2000; Sigma) and anti-Myc antibody (1:2000; Sigma). The membranes were subsequently incubated for 1 h with anti-mouse or anti-rabbit horseradish peroxidase (HRP)-conjugated secondary antibody (1:2000; Cell Signalling Technology), and the signal was detected using an ECL Western Blotting Detection System (GE Healthcare).

### 4.4 | Yeast two-hybrid and BiFC assays

To analyse the interactions of CIPK31 with other proteins, a MatchMaker yeast two-hybrid system (Y2H; Takara) was used. The complete, N-terminal, and C-terminal coding sequences of CIPK31 were subcloned into the pGBT9 (DNA-binding domain, BD) vector, and the coding sequences of the *RBOHs* (*RBOH A, B, C, D, E, H*) and *Catalases* (*CatA, CatB, and CatC*) were subcloned into pGAD424 (activation domain, AD). The recombinant AD and BD plasmid pairs were cotransformed into the yeast strain Y2HGold, following the yeast transformation protocol (Takara). The transformants were coated on nutrient-deficient medium plates SD/–Leu–Trp. A single colony was selected to put in a glass tube with SD/–Leu–Trp liquid medium and cultured on a shaker at 220 rpm. After 2–3 days, 5 µl culture solution were placed on SD/–Leu–Trp and SD/–Leu–Trp–His plates.

Primers used for Y2H are listed in Table S1.

The coding sequences of *CIPK31* and *CatC* were cloned into the fluorescent protein vectors pXNGW and pXCGW, and these constructs were cotransformed into *Nicotiana* leaves using *Agrobacterium tumefaciens* GV3101-mediated infiltration transformation (Kim et al., 2009). H2B-RFP was used as a nuclear marker, and pXNGW and pXCGW vectors with no target genes were used as the negative control. The fluorescence due to the yellow fluorescent protein (YFP) was detected using an Olympus confocal laser-scanning microscope after 48 h of infiltration.

### 4.5 | RNAi and overexpression vector construction

Three hundred base pairs of *RBOHA* and *CatC* cDNA fragments were cloned into the modified pBSK(+) vector (Biovector) with the β-glucuronidase gene (*GUS*) intron sequences in sense and antisense directions, and the sense-*GUS* intron-antisense fragment was subcloned into the pCAMBIA1381-*UBI* vector (Cambia) to generate the RNAi vectors. The open reading frame sequences of *CIPK31*, *RBOHA*, and *CatC* were cloned into pCAMBIA1381-*UBI* to generate the overexpression vector. The primers used for vector construction are listed in Table S1.

Rice transformation was carried out by using *Agrobacterium*-mediated methods in Zhonghua 11 (ZH11) japonica cultivar background (Nandi et al., 2000). The transformed plants were regenerated in the presence of hygromycin 50 mg/L and transferred to soil after 4 weeks of growth on Murashige and Skoog medium with hygromycin 50 mg/L.

### 4.6 | DAB staining and H<sub>2</sub>O<sub>2</sub> measurement

Neatly trimmed fresh leaf was immersed in a centrifuge tube containing DAB solution, with a three-quarter portion exposed to air. The tube was wrapped in aluminium foil and incubated at 37°C for 12–18 h. The tube containing the sample was then dehydrated with



90% ethanol solution in a water bath kettle for 2–3 h. After complete decolorization, the leaf samples were put into fresh 90% ethanol solution, cooled, and observed.

The H<sub>2</sub>O<sub>2</sub> concentrations were measured using an assay kit (Nanjing Jiancheng Bioengineering Institute), following the manufacturer's instructions. The leaf samples were weighed and put in a mortar. Nine times the weight of sample of (1:9 wt/vol) phosphate-buffered saline (pH 7.0–7.4) was added. The samples were ground under ice bath conditions then centrifuged at 1000×g for 10 min. The absorbance of the supernatant was examined by spectrophotometer UV752 (Yoke) at 405 nm. The control group included 0.1 ml of double-distilled water. The standard group included 0.1 ml of 163 mM H<sub>2</sub>O<sub>2</sub>. The content of H<sub>2</sub>O<sub>2</sub> (mmol/g protein) = [(A<sub>measure</sub> - A<sub>control</sub>/A<sub>standard</sub> - A<sub>control</sub>) × C<sub>standard</sub>]/C<sub>pr</sub>, where C<sub>pr</sub> is the protein concentration of tissue.

#### 4.7 | Measurement of catalase activity

The catalase (CAT) activity was measured using the Micro Catalase (CAT) assay kit (Solarbio), following the manufacturer's protocol. Two-week-old plants leaves were used for protein extraction and subsequent catalase activity calculation. Samples of 0.1 g of leaves were ground in 1 ml of abstraction solution in an ice bath then centrifuged at 8000×g, 4°C for 10 min. The absorbance of supernatant was examined by microplate reader at 240 nm, zero setting by using distilled water. CAT activity (U/g) = [ΔA × V<sub>total</sub> / (ε × d) × 10<sup>6</sup>] / (V<sub>sample</sub> / V<sub>total sample</sub> × W) / T, where V<sub>total</sub> is the total volume of the reaction system (2 × 10<sup>-4</sup> L), ε is the H<sub>2</sub>O<sub>2</sub> molar extinction coefficient (43.6 L/mol/cm), d is the optical path of the 96-well plate (0.6 cm), V<sub>sample</sub> is the sample volume (0.01 ml), V<sub>total sample</sub> is the volume of extraction solution (1 ml), T is the reaction time (1 min), and W is the sample weight (g).

#### 4.8 | Simulation models of protein interactions

The amino acid sequences of rice CIPK31, CatC, and RBOHA were downloaded from UniProt. The open-source AF2 complex (<https://github.com/FreshAirTonight/af2complex>) predictive analysis system was used to predict the protein interaction model (Gao et al., 2022).

#### 4.9 | Recombinant protein expression

To produce GST or NAF-GST recombinant proteins, NAF domain region sequences were subcloned into the pGEX5×-1 expression vector, and the resulting pGEX5×-1-NAF plasmid was used for transformation of *E. coli* BL21 (DE3). Recombinant proteins were harvested after 4 h of 0.5 mM isopropyl-β-D-thiogalactopyranoside (IPTG) treatment at 37°C.

#### 4.10 | Statistical analysis

Statistical analysis was performed using Prism 8 (GraphPad). All data were expressed as mean ± SE (n = 3). Student's *t* test was used to compare and determine statistically significant differences between the two groups. A one-way analysis of variance (ANOVA) was used to compare more than two groups. The *t* test and ANOVA were followed by Bonferroni's multiple comparison tests. The differences among the samples were considered significant at *p* < 0.05.

#### ACKNOWLEDGEMENTS

This work was supported by the Nature Science Foundation of Liaoning (2020-YQ-05), the Nature Science Foundation of China (32072406) and the open project from State Key Laboratory for Exploitation and Utilization of Crop Genetic Resources in Southwest China (SKL-KF202220) and Nature Science Foundation of Liaoning (2022-BS-173). We thank Professor Chang-Deok Han from Gyeongsang National University for providing the *Ds*-insertional mutants, and Professor Yuese Ning from the Institute of Plant Protection, Chinese Academy of Agricultural Science for providing the *voz2* T-DNA mutant. We also thank Professor Shimin Zuo from Yangzhou University for providing Hap\_2 cultivar seeds and Professor Jian Sun from Shenyang Agricultural University for providing Hap\_1 cultivar seeds.

#### CONFLICT OF INTEREST

The authors declare no conflict of interest.

#### DATA AVAILABILITY STATEMENT

Data is available from the corresponding author.

#### ORCID

Yuanhu Xuan  <https://orcid.org/0000-0002-4704-8090>

#### REFERENCES

- Cao, W., Zhang, H., Zhou, Y., Zhao, J., Lu, S., Wang, X. et al. (2021) Suppressing chlorophyll degradation by silencing OsNYC3 improves rice resistance to *Rhizoctonia solani*, the causal agent of sheath blight. *Plant Biotechnology Journal*, 20, 335–349.
- Cho, C., Kim, K.H., Choi, M.-S., Chun, J., Seo, M.-S., Jeong, N. et al. (2019) Characterization of a gamma radiation-induced salt-tolerant silage maize mutant. *Korean Society of Breeding Science*, 51, 318–325.
- Eizenga, G.C., Prasad, B., Jackson, A.K. & Jia, M.H. (2013) Identification of rice sheath blight and blast quantitative trait loci in two different *O. sativa*/*O. nivara* advanced backcross populations. *Molecular Breeding*, 31, 889–907.
- Gao, M., He, Y., Yin, X., Zhong, X., Yan, B., Wu, Y. et al. (2021) Ca<sup>2+</sup> sensor-mediated ROS scavenging suppresses rice immunity and is exploited by a fungal effector. *Cell*, 184, 5391–5404.e5317.
- Gao, M., Nakajima An, D., Parks, J.M. & Skolnick, J. (2022) AF2Complex predicts direct physical interactions in multimeric proteins with deep learning. *Nature Communications*, 13, 1744.

- Groom, Q.J., Torres, M.A., Fordham-Skelton, A.P., Hammond-Kosack, K.E., Robinson, N.J. & Jones, J.D. (1996) *rbohA*, a rice homologue of the mammalian *gp91phox* respiratory burst oxidase gene. *The Plant Journal*, 10, 515–522.
- Han, J.P., Köster, P., Drerup, M.M., Scholz, M., Li, S., Edel, K.H. et al. (2019) Fine-tuning of RBOHF activity is achieved by differential phosphorylation and Ca<sup>2+</sup> binding. *New Phytologist*, 221, 1935–1949.
- Hao, M.S. & Rasmusson, A.G. (2016) The evolution of substrate specificity-associated residues and Ca<sup>2+</sup>-binding motifs in EF-hand-containing type II NAD(P)H dehydrogenases. *Physiologia Plantarum*, 157, 338–351.
- Helliwell, E.E., Wang, Q. & Yang, Y. (2013) Transgenic rice with inducible ethylene production exhibits broad-spectrum disease resistance to the fungal pathogens *Magnaporthe oryzae* and *Rhizoctonia solani*. *Plant Biotechnology Journal*, 11, 33–42.
- Kim, J.G., Li, X., Roden, J.A., Taylor, K.W., Aakre, C.D., Su, B. et al. (2009) *Xanthomonas* T3S effector XopN suppresses PAMP-triggered immunity and interacts with a tomato atypical receptor-like kinase and TFT1. *The Plant Cell*, 21, 1305–1323.
- Kurusu, T., Hamada, J., Nokajima, H., Kitagawa, Y., Kiyoduka, M., Takahashi, A. et al. (2010) Regulation of microbe-associated molecular pattern-induced hypersensitive cell death, phytoalexin production, and defense gene expression by calcineurin B-like protein-interacting protein kinases, OsCIPK14/15, in rice cultured cells. *Plant Physiology*, 153, 678–692.
- Li, N., Lin, B., Wang, H., Li, X., Yang, F., Ding, X. et al. (2019) Natural variation in ZmFBL41 confers banded leaf and sheath blight resistance in maize. *Nature Genetics*, 51, 1540–1548.
- Lin, A., Wang, Y., Tang, J., Xue, P., Li, C., Liu, L. et al. (2012) Nitric oxide and protein S-nitrosylation are integral to hydrogen peroxide-induced leaf cell death in rice. *Plant Physiology*, 158, 451–464.
- Lin, Q.J., Kumar, V., Chu, J., Li, Z.M., Wu, X.X., Dong, H. et al. (2021) CBL-interacting protein kinase 31 regulates rice resistance to blast disease by modulating cellular potassium levels. *Biochemical and Biophysical Research Communications*, 563, 23–30.
- Liu, J.M., Mei, Q., Yun Xue, C., Yuan Wang, Z., Pin Li, D., Xin Zhang, Y. et al. (2021) Mutation of G-protein  $\gamma$  subunit DEP1 increases planting density and resistance to sheath blight disease in rice. *Plant Biotechnology Journal*, 19, 418–420.
- Liu, P., Duan, Y., Liu, C., Xue, Q., Guo, J., Qi, T. et al. (2018) The calcium sensor TaCBL4 and its interacting protein TaCIPK5 are required for wheat resistance to stripe rust fungus. *Journal of Experimental Botany*, 69, 4443–4457.
- Liu, P., Guo, J., Zhang, R., Zhao, J., Liu, C., Qi, T. et al. (2019) TaCIPK10 interacts with and phosphorylates TaNH2 to activate wheat defense responses to stripe rust. *Plant Biotechnology Journal*, 17, 956–968.
- Molla, K.A., Karmakar, S., Molla, J., Bajaj, P., Varshney, R.K., Datta, S.K. et al. (2020) Understanding sheath blight resistance in rice: the road behind and the road ahead. *Plant Biotechnology Journal*, 18, 895–915.
- Nagano, M., Ishikawa, T., Fujiwara, M., Fukao, Y., Kawano, Y., Kawai-Yamada, M. et al. (2016) Plasma membrane microdomains are essential for Rac1-RbohB/H-mediated immunity in rice. *The Plant Cell*, 28, 1966–1983.
- Nagarjuna, K., Parvathi, M., Sajeevan, R., Pruthvi, V., Mamrutha, H. & Nataraja, K. (2016) Full-length cloning and characterization of abiotic stress responsive CIPK31-like gene from finger millet, a drought-tolerant crop. *Current Science*, 111, 890–894.
- Nandi, A.K., Kushalappa, K., Prasad, K. & Vijayraghavan, U. (2000) A conserved function for *Arabidopsis* SUPERMAN in regulating floral-whorl cell proliferation in rice, a monocotyledonous plant. *Current Biology*, 10, 215–218.
- Peng, Y., Hou, F., Bai, Q., Xu, P., Liao, Y., Zhang, H. et al. (2018) Rice calcineurin B-like protein-interacting protein kinase 31 (OsCIPK31) is involved in the development of panicle apical spikelets. *Frontiers in Plant Science*, 9, 1661.
- Piao, H.-l., Xuan, Y.-h., Park, S.H., Je, B.I., Park, S.J., Park, S.H. et al. (2010) OsCIPK31, a CBL-interacting protein kinase is involved in germination and seedling growth under abiotic stress conditions in rice plants. *Molecules and Cells*, 30, 19–27.
- Pinson, S., Capdevielle, F.M. & Oard, J.H. (2005) Confirming QTLs and finding additional loci conditioning sheath blight resistance in rice using recombinant inbred lines. *Crop Science*, 45, 503–510.
- Qi, L., Zhang, T., Zeng, J., Li, C., Li, T., Zhao, Y. et al. (2021) Analysis of the occurrence and control of diseases in five major rice-producing areas in China in recent years. *China Plant Protection*, 41, 37–42.
- Richa, K., Tiwari, I.M., Devanna, B.N., Botella, J.R., Sharma, V. & Sharma, T.R. (2017) Novel chitinase gene LOC\_Os11g47510 from indica rice Tetep provides enhanced resistance against sheath blight pathogen *Rhizoctonia solani* in rice. *Frontiers in Plant Science*, 8, 596.
- Richa, K., Tiwari, I.M., Kumari, M., Devanna, B.N., Sonah, H., Kumari, A. et al. (2016) Functional characterization of novel chitinase genes present in the sheath blight resistance QTL: qSBR11-1 in rice line Tetep. *Frontiers in Plant Science*, 7, 244.
- Sardar, A., Nandi, A.K. & Chattopadhyay, D. (2017) CBL-interacting protein kinase 6 negatively regulates immune response to *Pseudomonas syringae* in *Arabidopsis*. *Journal of Experimental Botany*, 68, 3573–3584.
- Shi, X., Long, Y., He, F., Zhang, C., Wang, R., Zhang, T. et al. (2018) The fungal pathogen *Magnaporthe oryzae* suppresses innate immunity by modulating a host potassium channel. *PLoS Pathogens*, 14, e1006878.
- Sun, Q., Li, D.D., Chu, J., Yuan, P., Li, S., Zhong, L.J. et al. (2020) Indeterminate domain proteins regulate rice defense to sheath blight disease. *Rice*, 13, 15.
- Sun, Q., Li, T.Y., Li, D.D., Wang, Z.Y., Li, S., Li, D.P. et al. (2019a) Overexpression of loose plant architecture 1 increases planting density and resistance to sheath blight disease via activation of PIN-FORMED 1a in rice. *Plant Biotechnology Journal*, 17, 855–857.
- Sun, Q., Liu, Y., Wang, Z.Y., Li, S., Ye, L., Xie, J.X. et al. (2019b) Isolation and characterization of genes related to sheath blight resistance via the tagging of mutants in rice. *Plant Gene*, 19, 100200.
- Tung, B.T., Rodriguez-Bies, E., Thanh, H.N., Le-Thi-Thu, H., Navas, P., Sanchez, V.M. et al. (2015) Organ and tissue-dependent effect of resveratrol and exercise on antioxidant defenses of old mice. *Aging Clinical and Experimental Research*, 27, 775–783.
- Wang, W., Mauleon, R., Hu, Z., Chebotarov, D., Tai, S., Wu, Z. et al. (2018) Genomic variation in 3,010 diverse accessions of Asian cultivated rice. *Nature*, 557, 43–49.
- Xue, X., Cao, Z.X., Zhang, X.T., Wang, Y., Zhang, Y.F., Chen, Z.X. et al. (2016) Overexpression of OsOSM1 enhances resistance to rice sheath blight. *Plant Disease*, 100, 1634–1642.
- Yang, C., Li, W., Cao, J., Meng, F., Yu, Y., Huang, J. et al. (2017) Activation of ethylene signaling pathways enhances disease resistance by regulating ROS and phytoalexin production in rice. *The Plant Journal*, 89, 338–353.
- You, X., Zhang, F., Liu, Z., Wang, M., Xu, X., He, F. et al. (2022) Rice catalase OsCATC is degraded by E3 ligase APIP6 to negatively regulate immunity. *Plant Physiology*, 190, 1095–1099.
- Yuan, D.P., Xu, X.F., Hong, W.-J., Wang, S.T., Jia, X.T., Liu, Y. et al. (2020) Transcriptome analysis of rice leaves in response to *Rhizoctonia solani* infection and reveals a novel regulatory mechanism. *Plant Biotechnology Reports*, 14, 559–573.
- Yuan, P., Jauregui, E., Du, L., Tanaka, K. & Poovaiah, B.W. (2017) Calcium signatures and signaling events orchestrate plant-microbe interactions. *Current Opinion in Plant Biology*, 38, 173–183.
- Yuan, P., Zhang, C., Wang, Z.Y., Zhu, X.F. & Xuan, Y.H. (2018) RAVL1 activates brassinosteroids and ethylene signaling to modulate

response to sheath blight disease in rice. *Phytopathology*, 108, 1104–1113.

Zheng, A., Lin, R., Zhang, D., Qin, P., Xu, L., Ai, P. et al. (2013) The evolution and pathogenic mechanisms of the rice sheath blight pathogen. *Nature Communications*, 4, 1424.

#### SUPPORTING INFORMATION

Additional supporting information can be found online in the Supporting Information section at the end of this article.

**How to cite this article:** Chen, H., Lin, Q., Li, Z., Chu, J., Dong, H. & Mei, Q. et al. (2023) Calcineurin B-like interacting protein kinase 31 confers resistance to sheath blight via modulation of ROS homeostasis in rice. *Molecular Plant Pathology*, 24, 221–231. Available from: <https://doi.org/10.1111/mpp.13291>